

# SAMPLING AND ANALYSIS OF IMPACT CRATER RESIDUES FOUND ON THE WIDE FIELD PLANETARY CAMERA-2 RADIATOR

P. D. Anz-Meador<sup>(1)</sup>, J.-C. Liou<sup>(2)</sup>, D. Ross<sup>(1)</sup>, G. A. Robinson<sup>(1)</sup>, J. N. Opiela<sup>(1)</sup>, A. T. Kearsley<sup>(3)</sup>, G. W. Grime<sup>(4)</sup>, J. L. Colaux<sup>(4)</sup>, C. Jeynes<sup>(4)</sup>, V. V. Palitsin<sup>(4)</sup>, R.P. Webb<sup>(4)</sup>, T. J. Griffin<sup>(5)</sup>, B. B. Reed<sup>(5)</sup>, L. Gerlach<sup>(6)</sup>

<sup>(1)</sup> ESCG-Jacobs, Houston, Texas, USA. <sup>(2)</sup> NASA Johnson Space Center (JSC), Houston, Texas, USA.

<sup>(3)</sup> Science Facilities, Natural History Museum (NHM), London, United Kingdom, Email: [antk@nhm.ac.uk](mailto:antk@nhm.ac.uk)

<sup>(4)</sup> Ion Beam Centre (IBC), University of Surrey, Guildford, United Kingdom

<sup>(5)</sup> NASA Goddard Space Flight Center (GSFC), Greenbelt, Maryland, USA.

<sup>(6)</sup> European Space Agency (ESA, retired), Noordwijk, The Netherlands.

## ABSTRACT

After nearly 16 years in low Earth orbit (LEO), the Wide Field Planetary Camera-2 (WFPC2) was recovered from the Hubble Space Telescope (HST) in May 2009, during the 12 day shuttle mission designated STS-125. The WFPC-2 radiator had been struck by approximately 700 impactors producing crater features 300  $\mu\text{m}$  and larger in size. Following optical inspection in 2009, agreement was reached for joint NASA-ESA study of crater residues, in 2011. Over 480 impact features were extracted at NASA Johnson Space Center's (JSC) Space Exposed Hardware clean-room and curation facility during 2012, and were shared between NASA and ESA. We describe analyses conducted using scanning electron microscopy (SEM) - energy dispersive X-ray spectrometry (EDX): by NASA at JSC's Astromaterials Research and Exploration Science (ARES) Division; and for ESA at the Natural History Museum (NHM), with Ion beam analysis (IBA) using a scanned proton microbeam at the University of Surrey Ion Beam Centre (IBC).

## 1 INTRODUCTION

### 1.1 The importance of the WFPC2 radiator

The HST was deployed during the STS-31 mission in April 1990. Its initial orbit was 610 km by 618 km, with an inclination of 28.5°. Due to problems in the optical system, the original Wide Field Planetary Camera (WFPC) was replaced by WFPC2 in December 1993. This new camera was the "workhorse" instrument behind nearly all of the most famous HST celestial images released in the last decade. After more than 15 years of collecting invaluable data for astronomers around the world, WFPC2 was replaced by Wide Field Camera 3 (WFC3) during the final HST Servicing Mission 4 in May 2009. The entire WFPC2 instrument package was retrieved by the Atlantis astronauts and brought back to NASA.

The radiator attached to the WFPC2 camera was exposed to space for 15.5 years. Its dimensions are 0.8 m  $\times$  2.2 m; the outermost layer is a curved aluminum plate with a thickness of 4.06 mm.

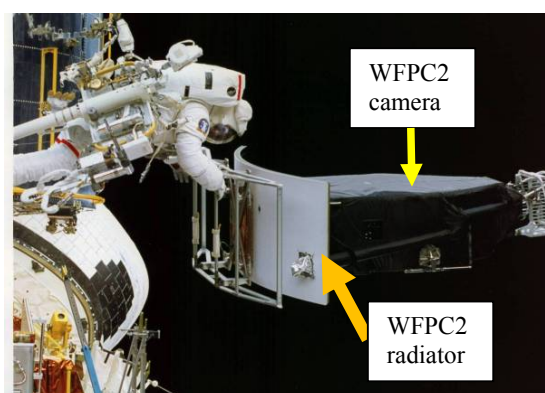


Figure 1. The WFPC2 being installed aboard HST during 1993's Servicing Mission (SM1).

The surface of the plate is covered with YB-71 white paint (Zinc Orthotitanate coating, or ZOT, a type of ceramic thermal control paint). The thickness of the paint varies across the surface, and is approximately between 100 and 200  $\mu\text{m}$ . Due to its large surface area and long exposure time, the radiator surface served as a unique witness plate for the micrometeoroid (MM) and orbital debris (OD) impacts at the HST altitude between 1993 and 2009. Because of high impact speed in space, 200  $\mu\text{m}$  and larger MM or OD particles could be a safety concern for human spaceflight and robotic missions in low Earth orbit (LEO, the region below 2000 km altitude). Since ground-based telescopes and radars are limited to the detection of particles several millimeters and larger in space, the WFPC2 impact data are key to provide information on the millimeter and smaller MM and OD populations in LEO.

### 1.2 Optical inspections

After STS-31, the surface of WFPC was examined for impact features, although little analytical work to determine impactor origins as MM or OD was performed [1]. The post-flight optical examination of the WFPC2 radiator took place over six weeks during the summer of 2009 in the NASA GSFC "White House" Class 100k clean room. This examination recorded details about all micrometeoroid and orbital debris (MMOD) impact features with diameters of 300

$\mu\text{m}$  or larger. Using a laser pattern projector and digital microscope, team members from two NASA centers recorded the positions, diameters, and depths of each of 677 craters. The digital microscope allowed the team to record crater images and image properties, then extract the actual measurements later in an office environment. Results of the optical survey have already been presented [2] and published as a NASA Technical Publication [3]. A significant finding is that 74% of the craters did not penetrate the layer of white paint on the outside of the radiator panel. During the 2009 optical inspection of the radiator, some features thought to be interesting but of non-impact origin were also recorded, usually with fewer than three images and no depth information. The survey did not record all non-impact features, but only unique items or examples representative of a class. About 54% of the recorded features were found to be surface contamination. Non-crater paint damage (e.g., divots, scratches and dents) and apparent paint defects each made up about 8% of the non-impact features. Of the surface contaminants, 60% were objects on the surface and 40% were spots, stains, and smudges. About 30% of the total number were found to be sub-threshold (i.e.,  $<300\ \mu\text{m}$ ) craters and apparent (though unusual in appearance) craters.

### 1.3 Radiator custody & handling

In November 2009, the WFPC2 was shipped to the Smithsonian National Air & Space Museum for display; it was also displayed at NASA Jet Propulsion Laboratory and the Denver Museum of Nature and Science before returning to storage in November 2010. During this time, the WFPC2 was enclosed by a transparent cover over the WFC3 shipping container base. The container was not purged and was not airtight. The radiator was de-integrated from the camera assembly in September 2011 in GSFC's Laurel (Maryland) warehouse and bagged in Llumalloy sheets for shipment to JSC in December 2011. During bagging, the radiator was exposed to the ambient warehouse environment. After its arrival at JSC, the radiator assembly was inserted into the Space Exposed Hardware (SEH) Class 10k cleanroom for coring.

## 2 THE JOINT ESA-NASA EFFORT

The Hubble Space Telescope Project has been operated as an ESA/NASA partnership since its inception in the mid-1980s. It is considered one of NASA's most successful international partnerships, forging a consolidated team of dedicated scientists and engineers to develop the Observatory and execute six extremely complicated and successful space shuttle missions. This relationship is ever evolving as ESA and NASA scientists continue to expand our knowledge of the

Universe.

The most recent collaboration has been focused on studying the WFPC2. The WFPC2 science instrument was removed from the HST Observatory in 2009 during the fifth and final HST Servicing Mission, designated HST SM-4. This instrument was installed during the first servicing mission, HST SM-1, in 1993. With its long duration on orbit life time, NASA was interested in the space environment effects on the optics as well as the micro-meteorite impacts on the external radiator. Initial steps to preserve the artifacts were taken soon after the Space Shuttle, Endeavour, was returned to NASA Kennedy Space Center.

Subsequent investigations were proposed whose methodology would take advantage of scientific techniques employed in previous HST Solar Array impact studies performed by ESA. NASA approached ESA to consider performing impact analyses on the WFPC2 radiator impact sites. ESA agreed and the international team developed a joint ESA/NASA investigation plan where impact samples would be studied both in Europe and in the United States. This report summarizes the initial results of that investigation.

Detailed discussion of our joint findings remains premature at this point. Here we explain the methods adopted for sample preparation, handling, analysis and interpretation. In particular we describe development of a core sampling technique; the practical taxonomy developed to classify residues as belonging either to anthropogenic orbital debris or micrometeoroids of natural origin; and the protocols for examination of crater residues. Challenges addressed in sample extraction were the relative thickness of the surface to be cut, protection of the impact feature from contamination while coring, and the need to preserve the cleanroom environment so as to preclude or minimize cross-contamination. We summarise impactor classification criteria, including the recognition and assessment of surface contamination, and the necessity for surface cleaning.

In this paper, we discuss analytical techniques used to examine the crater residues: EDX from either electron excitation (SEM-EDX) and, for cores assessed as "difficult" targets, proton excitation (IBA). All samples were documented by electron imagery: backscattered electron imagery in the SEM, and where appropriate, secondary electron imagery during IBA.

## 3 SAMPLING THE RADIATOR SURFACE

### 3.1 Coring Techniques

Collecting samples from the thick surface using a core drill presented itself as the technique offering greatest

probability of success, within two major constraints: not contaminating the sample during collection, and not compromising the integrity of the cleanroom in which sampling would be conducted. A novel, unique sampling tool was developed to perform cleanroom coring of the WFPC2 impact features. This annular cutter is shown in Figure 2, along with its products.

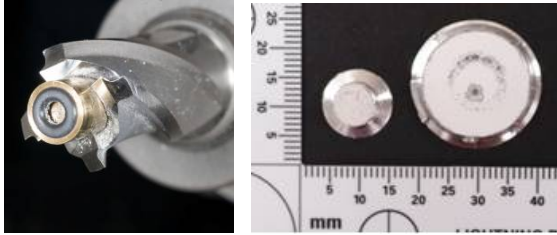


Figure 2. (left) the coring device developed at JSC. (right) Exemplar cores taken with the small and large cutters. The small core is a reference standard.

In this case, a standard 5/8 inch (~ 16 mm) outer diameter tool steel cutting tool was modified with a concentric, spring-loaded, phosphor-bronze cylinder. The cylinder is tipped with a standard Viton O-ring to protect the feature being cored. As the core drill is brought into contact with the radiator's surface, friction between the surface and the O-ring brings the cylinder to rest within the rotating annular cutter. As the cutter is advanced into the surface the cylinder retracts into the hollow core of the cutting tool, allowing the radiator's Aluminum substrate to be cut while protecting the feature of interest. The O-ring was changed regularly to minimize contamination or cross-contamination of the surface. A larger 1-1/16<sup>th</sup> inch (~ 27 mm) diameter cutting tool was similarly modified, to allow larger craters or those displaying areas of paint spallation to be collected.

The core drill motor was mounted on a four degree of freedom assembly derived from commercial machine shop components and was capable of vertical, lateral, plunging, and rotational motion. The latter was required by the curved surface of the radiator, and care was taken to enter the radiator at normal incidence. The feature to be cored was identified by eye and the core drill was coarsely aligned using the fixture. Fine alignment was provided by a commercial laser projection system, and the fixture adjusted accordingly to place a laser "X" over the target feature.

A commercial drill dust catcher was modified with a custom, 3D printed ceramic base; the base touched the surface of the radiator only with a Viton O-ring. Together these formed a vacuum shroud; the shroud is ducted to a High Efficiency Particulate Air (HEPA)-filtered cleanroom vacuum. Dust generated by cutting is collected by the vacuum while larger strands of Aluminum and ZOT chips are collected by the shroud assembly itself.

The technique proved highly successful, producing samples which could be handled safely and without significant detachment of the thin paint layer.

### 3.2 Inventory of cores

A total of 486 large and small cores were collected. After inspection by coring team members, each was assigned a sequential serial number, marked on base or lateral surface area. The cores were then placed in an Al-6061 rack for storage and shipment. The rack holds the cores firmly within Teflon O-rings, thereby protecting and isolating each impacted surface. Random selection was used to ensure both the NASA JSC and ESA teams received features of all sizes and locations from the radiator's surface.

### 3.3 Surface contamination

Radiator surface contamination had been noted prior to our 2009 optical survey. Some cores indeed proved merely to sample surface contaminants rather than impact features. After preliminary identification, these were not analysed further. Between coring sessions the radiator was draped in its Llumalloy shipping bag to minimize particulate fall onto the surface. Use of O-ring seals (with repeated renewal), and the HEPA vacuum shroud minimized contamination of the surface and impact features. However, the Viton O-rings did leave some F-bearing polymeric materials on the core surface over their contact area. The vacuum shroud was not entirely successful in protecting features below that being cored from the fall of Al/paint dust, but loose contamination was easily removed. Surface particulates found around impact features, but not in their impact melts, also included the elements: Ag, Bi, Sn, Cd, Er, Ce, FeCrNi, PbCuZn, W, FeWVCr (coring tool), MgP, MgCrPNa, BaSO, CaP, Ni, MoFe, and AgS.

Many samples revealed the presence of a K-rich material at the surface, also containing oxygen and carbon. Laser Raman spectroscopy showed this to be KHCO<sub>3</sub> (potassium hydrocarbonate). It was sometimes present as large surface patches, or as needles that are very sensitive to damage during exposure to an electron beam and move during examination, contributing to charging issues that complicate imaging. KHCO<sub>3</sub> fills large portions of some craters, clearly being formed post-impact, and hindered observation and X-ray data collection. The phase is very soluble, and some craters were treated with distilled water, in order to remove this material, which we consider to be an ageing product of the paint binder composition.

## 4 IMPACTOR CLASSIFICATION

Our aim was to find diagnostic impact residue compositions and use them to recognize particle origins. Analytical data from the impact feature would reveal those elements which were either not expected in the radiator (i.e. undoubtedly of extraneous origin), or were detected at anomalous levels. Such an approach must take into account the specific localised substrate for each individual impact, and it was critical to have a detailed understanding of the structure and composition of all components in the radiator before attempting to classify impactor type and origin. This was an early objective of our work, as explained in 5.3 below.

Some elemental combinations give rapid and unambiguous recognition of impactor. E.g. co-location of Mg, Si, Fe and O in an impact feature on a substrate which does not contain these elements is a reliable indication of mafic silicate impact [4], the most abundant type of MM [5]. Unfortunately, the WFPC2 composition precludes recognition of some impactors, as their residues cannot be distinguished from components already present in the radiator.

i) MM – the silicate, sulfide, oxide and carbonate minerals, amorphous mafic silicate glass and variable amounts of organic material are distinctive [6] and do not resemble artificial materials employed in orbital operations. There are no reported aerospace applications of iron sulfides, magnesium silicates or phyllosilicates, which make up the bulk of MM. Meteoritic Fe metals have relatively high Ni [5], with low Cr and Mn levels, easy to distinguish from ferrous alloys. Residues containing a substantial proportion of MM materials might therefore be relatively easy to tell apart from the WFPC2 components.

ii) OD – although a wide range of materials are employed in aerospace applications, previous studies [e.g. 6] have shown that several dominate: Al alloys, usually with Mg and Cu, and containing  $\mu\text{m}$ -scale inclusions of Mg, Si, Fe, Cr, Mn (and occasionally Ni); ferrous alloys containing either Cr or both Cr and Ni ('stainless steels'); specialised alloys; paint particles containing organic or silicate binder and Zn or Ti oxide pigments; Al or Al oxide from solid rocket motor operations; and alkali metal Na/K droplets. Unfortunately, Al, Zn and Ti (which are likely to be among the most common types of anthropogenic OD) cannot be reliably assigned as impacting elements on WFPC2 because of their abundance in the radiator materials. More exotic reported OD compositions have included solders and electronic components, and polymeric materials released from disruption of orbiting craft. Although Al oxides are found as very rare grains in meteoritic materials [5], none of the other OD would be easily confused with MM.

To standardise the process of impactor attribution, we

used discriminatory flow diagrams (e.g. Fig. 3) to sequentially exclude different types of material.

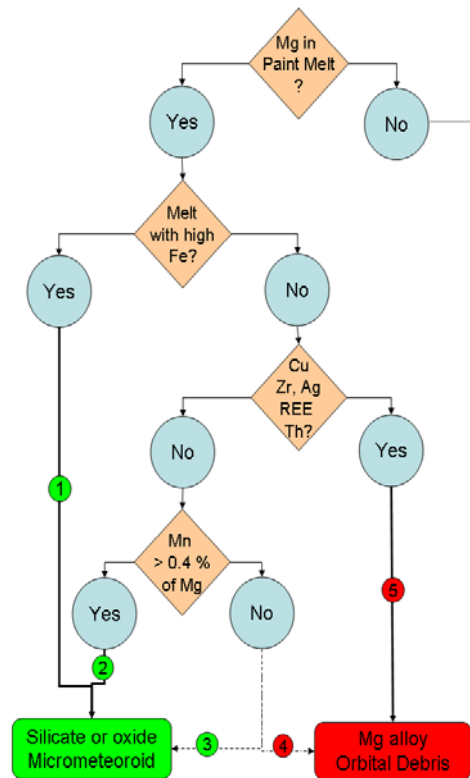


Figure 3. Example: Mg-rich residue classification

## 5 EXAMINATION OF THE SAMPLES

### 5.1 Analytical Methods

Scanning Electron Microscopy and Energy Dispersive X-ray Microanalysis (SEM-EDX) were used at JSC and NHM. These techniques are long established in analysis of hypervelocity impact residues [e.g. 8-13], and recent instrument developments allow rapid acquisition of elemental data from carefully chosen areas of the impact features, especially where melt textures were found (Fig. 4). The reliability of impactor determination by SEM-EDX of residue has been verified by experimental analogue studies [e.g. 14]. In this study, stereo imagery and construction of digital elevation models were used to measure impact feature depth and volume (Fig. 4). Automated X-ray mapping was also used to locate widely spaced patches of extraneous composition and surface contaminant grains. Most impact features yielded diagnostic information in EDX spectra (e.g. Fig. 5), but in cases where the radiator materials appeared to dominate the melt composition, more sensitive ion beam analysis techniques were also used. Particle Induced X-ray Emission (PIXE) was performed using the Tandetrion

2.5 MeV proton beam line at the Ion Beam Centre (IBC) of the University of Surrey, at Guildford (UK). PIXE maps and spectra allowed spatial location of diagnostic elemental signatures at trace concentrations, both confirming SEM-EDX analyses of impactor residue within WFPC2 melted paint, and allowing recognition of the subtle transition metal contributions from the extraneous impactor composition even when mixed with WFPC2 alloy.

Before application to WFPC2, the analytical protocols were tested on a sample of ZOT-painted Al alloy sheet, impacted by an undisclosed projectile type at the NASA White Sands Test Facility (WSTF) hypervelocity impact facility. Both SEM-EDX and PIXE gave immediate (and correct) unambiguous identification of the projectiles as stainless steel.

### 5.2 JSC Case Study

Two instruments: a JEOL 7600F SEM, equipped with a ThermoScientific SD (silicon drift) X-ray detector; and a JEOL JSM-5910LV SEM, equipped with a ultrathin-window Si(Li) X-ray detector; were used to examine, image and obtain chemical analyses from the cored impact features, which were carbon coated to ensure conductivity. Secondary electron (SE) and backscattered electron images (BEI) were collected to permit measurement of crater sizes, and to search for unusual compositions. Regions within and near craters were searched in BEI (which may reveal compositional variation). Phases notably different in brightness in BEI were characterized for chemistry by collection of X-ray spectra. However, the complex character of the impacted surface, with Zn-orthotitanate and potassium silicate constituents, as well as substantial porosity, variable volatile element contents, and very irregular surface topography, gave very complex electron backscattering, rendering the search for distinctive impactor remnants by BEI difficult.

The X-ray analyses showed that melts derived from surface paint always contained Zn, Ti, K, Si and O. Al is also widely present in the paint, and very frequently found as a minor component in melts formed from paint. We also observed Al-rich particles within pore spaces in the paint layer, their origin is not yet resolved. Small areas of Mg enrichment were found in the paint, but without detectable Fe, and unlikely to be confused with residue from most mafic silicate MM grains.

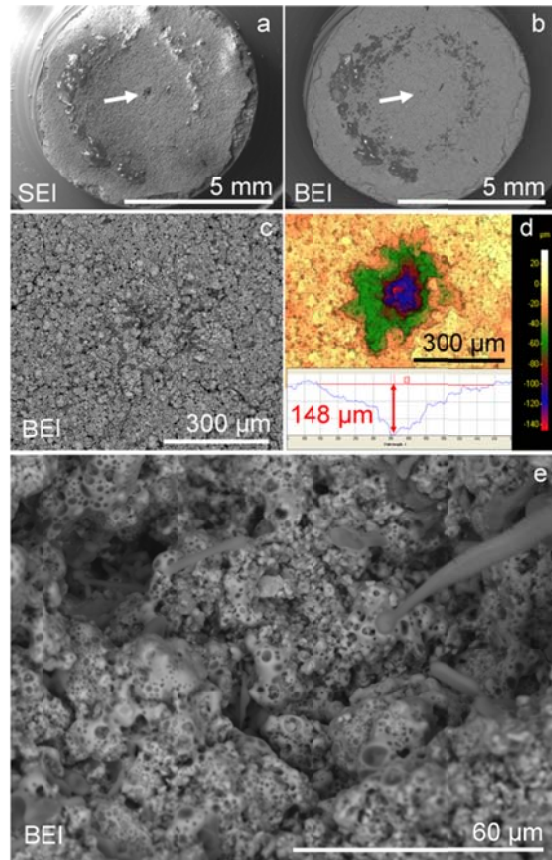


Figure 4. WFPC2 sample 97: a) Secondary (SEI) and b) Backscattered (BEI) electron images of a cored impact feature in the paint layer; c) BEI detail of impact; d) depth model and depth profile which shows that the crater did not penetrate into the underlying Al alloy; e) vesicular (bubbly) melt within the crater, containing residue from the impactor (see Fig. 5). Also note the elongate  $\text{KHCO}_3$  crystal at top right.

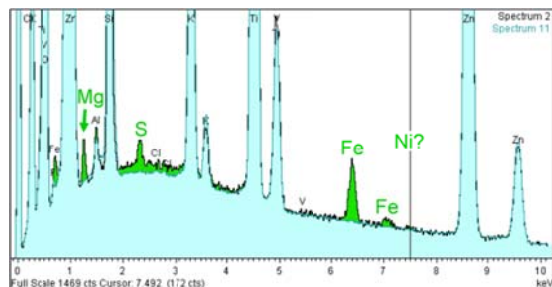


Figure 5. WFPC2-97. SEM-EDX spectrum of residue in vesicular melt (green) compared to surrounding WFPC2 paint (blue). Note Fe, Mg and S in residue.

### 5.3 NHM Case Study: WFPC2 radiator composition

A polished vertical section through a small core revealed the two layers (Fig. 6). Typical paint thickness is 150-200  $\mu\text{m}$ . Porous ZOT pigment grains are held in

a thin coating of Si-rich binder, with patches of K-rich phase, probably hydrocarbonate. The underlying Al alloy metal contains Mg and Cu, with  $\mu\text{m}$ -scale inclusions of Mg with Si, and Fe with Cr and Mn. Exposed surfaces of the interface between paint and alloy show abundant Fluorine.

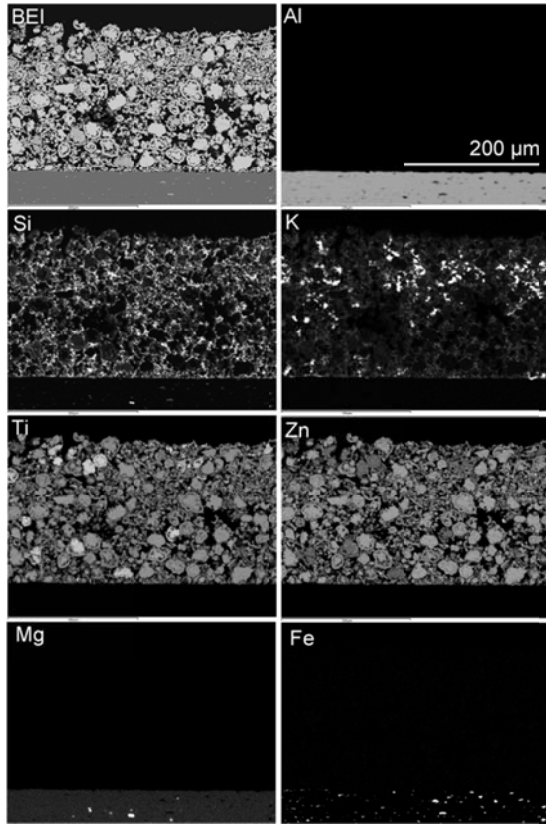


Figure 6. X-ray maps of a vertical section of WFPC2, note paint layer in the middle, and Al alloy at bottom.

From these features of the radiator, it was confirmed that several types of OD could not be reliably distinguished on WFPC2: Zn- and Ti- paints and K-rich coolant droplets. Where impacts penetrate to the alloy layer, the release of Al and inclusions is also problematic as this indigenous radiator material could be confused with traces of MM. Interpretation of Mg, Cr, Mn and Fe contents is then difficult unless very careful comparison of elemental abundance ratios is performed. Analysis by ion beam methods may therefore be necessary, to reveal the trace quantities of diagnostic transition metals.

#### 5.4 Preliminary results from impact features

Most smaller impact features of less than 500  $\mu\text{m}$  diameter (such as that illustrated in Figure 4) are confined to excavation of the paint layer, without revealing any of the alloy beneath. They usually yield

X-ray spectra that show clear signatures of the responsible impactor. Magnesium and iron enrichments are common in the vesicular melt, occasionally with minor calcium – these are probably derived from MM mafic silicates such as olivine and pyroxenes. Sulfur may also be present with Mg and Fe (e.g. Fig. 5), possibly as an original MM component (for example in either subsidiary sulfides or in layered oxide/sulfide/silicate). Fe and S may occur together, sometimes with Ni, suggesting an MM sulfide impactor. Al enrichment in melted paint (without incorporation from alloy beneath) coupled with Fe, Ni and Cu possibly indicates an OD alloy impact. In larger craters, which penetrate the alloy layer, unusual melt compositions included an example with high Cr as well as Mg, Al and Fe. Interpretation of this assemblage as of MM or OD origin requires careful consideration of the relative abundance of each element. Results from both SEM-EDX and PIXE show very high Cr relative to Fe, coupled with Mg enhancement relative to Al, and imply that this type of residue is not an alloy OD remnant, but more likely to be derived from impact of a MM Cr-rich spinel grain.

Our analysis of impact residues in the important larger features (e.g. Fig. 7) is still at a relatively early stage. We have found that these craters usually require cleaning, and then detailed searching to find melt textures, followed by acquisition of many long-duration EDX spectra acquisition or overnight X-ray mapping (Fig. 8) in order to locate areas that show unusual composition. Because the crater interior and surroundings are covered by a solidified melt composed mainly of alloy, mixed with varying quantities of ZOT paint, the signatures of an impactor are subtle and often require confirmation by IBA.

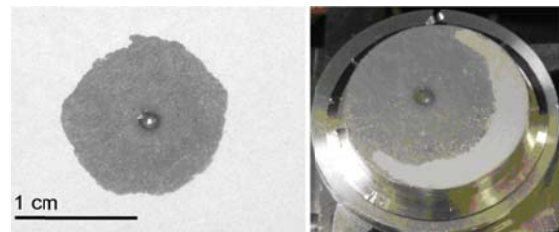


Figure 7. Optical photographs of feature 424, the largest impact on WFPC2, before and after removal as a core for microanalysis. Note the broad zone of spallation of the ZOT paint, surrounding a well-defined bowl-shaped central crater developed in the Al alloy.

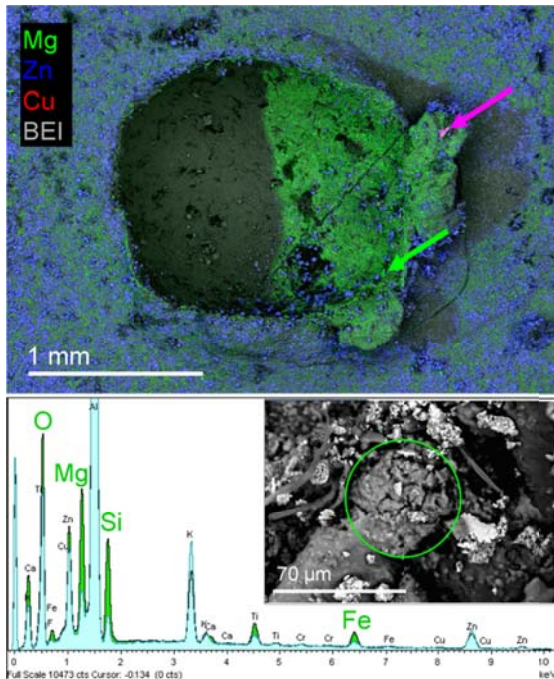


Figure 8. WFPC2 sample 424: a) combined false-colour X-ray maps for Mg (green), Zn (blue) and Cu (red) reveal Mg enrichment on the surface of the bowl-shaped crater, and a small shard of Cu-Zn alloy as a surface contaminant on the crater lip (pink arrow); b) BEI and X-ray spectrum (green) of an area rich in Mg, Fe, Si and O, probably a micrometeoroid remnant fused to the interior of the crater (spectrum in blue) at the location shown by the green arrow.

## 6. CURRENT STATUS AND FUTURE WORK

### 6.1 Sample examination and analysis

As of the beginning of March 2013, 195 cores had been examined at JSC, and 212 at NHM. A total of 357 impact features were found, imaged and analysed. About 40 samples remain to be examined. A suite of samples were documented and then exchanged between the laboratories, to test the correspondence between analytical protocols and data interpretation from the similar, but not identical instruments in the two laboratories. 25 samples were also submitted to IBC for further analysis, especially the comparison of minor and trace transition metal ratios. Analysis of the largest craters (about 25 samples) is still ongoing. Diagnostic residue is more difficult to find in these important features, and many will require very careful cleaning to reveal areas of impact melt. Their interior will be mapped using a new detector technology about to be installed at NHM, and by ion methods at IBC. Comparison of the full data sets, critical discussion of MM and OD identification criteria, and interpretation of impactor origins for almost 400 impact features should be completed in 2013.

### 6.2 Orbital Attitude, Facing Direction and the WFPC2 impact fluence

An activity parallel to that of the residue analyses is the assessment of HST pointing, and hence radiator attitude with respect to the spacecraft-centered local vertical-local horizontal (LVLH) coordinate frame. The OD population is highly directional in LVLH [e.g. 15], the MM population much less so [e.g. 16]. The GSFC HST Program Office has supplied JSC with 15 minute-cadence attitude data from 1993-2009, and the pointing distribution in LVLH over the WFPC2 exposure time is being determined. This work, in progress, will contribute to our understanding of the relative population statistics based on residue analysis.

### 6.3 The size of WFPC2 impactors, calibration by experiment and modelling

Inference of impactor size is complicated by the complex nature of the radiator's coated surface; prior work has interpreted impact features on uncoated materials, e.g. bare Al, Au, or on glass surfaces. To support the interpretation of WFPC2 impact features, two test programs have been conducted at WSTF. These tests impacted Al-6061 coupons painted with YB-71 thermal paint with a variety of projectile sizes and material types at speeds up to 7.9 km/s. The results of these test programs are being used to develop damage equations for the radiator, and will be extended to higher relative velocities using hydrocode modelling. When this work is completed in 2013, WFPC2 will yield the size distribution of the MMOD populations.

## 7. CONCLUSIONS

The WFPC2 radiator surface has preserved an unrivalled record of impacts in LEO. The large area-by-time product allowed the radiator surface to intercept a large number of hypervelocity particles during time in orbit. The relatively thick impact substrate (4 mm of Al alloy plate) prevented full penetration by even the largest impactor, thereby preserving information about an important part of the particle population that was not available from earlier studies of solar cell impacts (in which large impactors left little or no diagnostic trace [12]). The ZOT paint is a difficult substrate on which to perform analysis, may not reveal the presence of several important OD indicator elements (K, Ti and Zn), but is surprisingly efficient as a capture medium. The very distinctive vesicular impact melt texture gives an easy guide for locations of analysis. SEM-EDX and IBA of WFPC2 are yielding an unprecedented number of impactor identifications, and will reveal a significant data-set for modelling LEO particle populations.

## 8. ACKNOWLEDGEMENTS

Work at NHM and IBC was funded by ESA contract No. 4000105713/12/NL/GE.

## 9. REFERENCES

1. Humes, D.H. and Kinard, W.H. (1994). Meteoroid and Debris Impacts on the WF/PC I Radiator. HST Archive System, [http://setas-www.larc.nasa.gov/HUBBLE?PRESENTATIONS/hubble\\_talk\\_humes\\_kinard.html](http://setas-www.larc.nasa.gov/HUBBLE?PRESENTATIONS/hubble_talk_humes_kinard.html) (accessed 18th March 2013).
2. Opiela, J.N., Liou, J.-C., Anz-Meador, P.D., and Juarez, Q.L. (2010). Data Collected During the Post-Flight Survey of Micrometeoroid and Orbital Debris Impact Features on the Hubble Wide Field Planetary Camera 2. 61st International Astronautical Congress, Prague, CZ, 2010.
3. Opiela, J.N., Liou, J.-C., and Anz-Meador, P.D. (2012). Micrometeoroid and Orbital Debris Impact Feature Size and Position Data Collected During the Post-Flight Survey of the Hubble Wide Field Planetary Camera 2. NASA/TP-2012-217359.
4. Rietmeijer, F.J.R. and Blanford, G.E. (1988). Capture of an olivine micrometeoroid by spacecraft in low-Earth orbit. *J. Geophys. Res.* **93** (B10), 11943-11948.
5. Brearley, A.J. and Jones, R.H. (2000). Chondritic Meteorites. In: *Planetary Materials* (Ed. J.J Papike). Reviews in Mineralogy, **36**, Mineralogical Society of America.
6. Kearsley, A.T., Graham, G.A., McDonnell, J.A.M., Taylor, E.A., Drolshagen, G., Chater, R.J., McPhail, D. and Burchell, M.J. (2006). The chemical composition of micrometeoroids impacting upon the solar arrays of the Hubble Space Telescope. *Adv. Space Res.* **39**(4), 590-604.
7. Lurance, M.R & Brownlee, D.E. (1986). The flux of meteoroids and orbital space debris striking satellites in low Earth orbit. *Nature* **323**, 136-138.
8. Bernhard R. P., Durin, C. and Zolensky, M.E. (1993). Scanning electron microscope/energy dispersive X-ray analysis of impact residues in LDEF tray clamps. In: *LDEF - 69 Months in Space, Second Post-Retrieval Symposium*. (Ed. Levine A. S.), NASA Conference Publication 3194, NASA, Washington D.C., USA, 541-550.
9. Hörz, F., Bernhard, R.P., See, T.H. and Brownlee, D.E. 1995. Natural and Orbital Debris Particles on LDEF's Trailing and Forward-Facing Surfaces. In *LDEF - 69 Months in Space, Third LDEF Post-Retrieval Symposium* (Ed. A.S Levine), NASA Conference Publication 3275, NASA, Washington D.C., USA, pp415- 429.
10. Graham, G.A., Kearsley, A.T., Wright, I.P., Grady, M.M., Drolshagen, G., McBride, N.M., Green, S.F., Burchell, M.J., Yano, H. and Elliott, R. (2001). Analysis of impact residues on spacecraft surfaces: possibilities and problems. In *Proc. 3rd European Conference on Space Debris* (Ed. H. Sawaya-Lacoste), ESA SP-473. ESA Publications Division, European Space Agency, Noordwijk, The Netherlands.
11. Graham, G.A., McBride, Kearsley, A.T., Drolshagen, G., Green, S.F., McDonnell, J.A.M., Grady, M.M. & Wright, I.P. (2001). The chemistry of micrometeoroid and space debris remnants captured on the Hubble Space Telescope solar cells. *Int. J. Impact Eng.*, **26**, 263-274.
12. Kearsley, A.T. (2004). Analysis of Impact Residues on SM-3B HST Solar Arrays. Post-flight Impact Analysis of HST Solar Arrays - 2002 Retrieval. *Technical Note 3 for Contract No. 16283/NL/LvH*, submitted to European Space Agency (ESA/ESTEC).
13. Kearsley, A.T., Drolshagen, G., McDonnell, J.A.M., Mandeville, J.-C. & Moussi, A. (2005). Impacts on Hubble Space Telescope solar arrays: discrimination between natural and man-made particles. *Adv. Space Res.* **35**, 1254-1262.
14. Wozniakiewicz, P. J., Ishii, H. A., Kearsley, A. T., Burchell, M. J., Bradley, J. P., Price, M. C., Teslich, N., Lee, M. R. & Cole, M. J. (2012). Stardust Impact Analogues: Resolving Pre- and Post-Impact Mineralogy in Stardust Al Foils. *Meteorit. Planet. Sci.*, **47**, 708-728.
15. Hörz, F., Bernhard, R.P., See, T.H. & Kessler, D.J. (2002). Metallic and oxidized aluminum debris impacting the trailing edge of the Long Duration Exposure Facility (LDEF). *Space Debris*, **2**, 51-66.
16. See, T. H, Warren, J., Leago, K. & Zolensky, M. E. (1993). Particle flux as a function of pointing direction as determined from LDEF's structural components by the meteoroid and debris special investigation group. (Abstract) 3<sup>rd</sup> LDEF Post-retrieval symposium LDEF Washington D.C., NASA Conference Publication 10120: Meteoroids and Debris p45.

